LPV-model based identification approach of oscillatory failure cases

Andreas Varga and Daniel Ossmann

German Aerospace Center, DLR-Oberpfaffenhofen
Institute of Robotics and Mechatronics, D-82234 Wessling, Germany
(e-mail: {andreas.varga, daniel.ossmann}@dlr.de)

Abstract: The reliable early detection of *oscillatory failure cases* (OFC) for modern fly-by-wire controlled civil aircraft is an important aspect in optimizing the structural design objectives for reducing the environmental footprint of the aircraft. We propose a complete methodology for the design of a model based *fault detection and diagnosis* (FDD) system, which allows the reliable early detection of OFC characterized by low amplitude oscillations in a given frequency range. The main factors for the achieved enhanced performance are: the accurate modelling of the surface actuator via *linear parameter-varying* (LPV) models, an improved oscillation detection by employing the recursive discrete Fourier transform, and the integrated tuning of the free parameters of the FDD system using multi-objective optimization techniques.

Keywords: Fault detection, fault identification, analytical redundancy, oscillatory failure case.

1. INTRODUCTION

The identification of an *oscillatory failure case* (OFC) for a control surface is one of the best studied flight actuator failure cases in the literature (see Goupil (2010b) and references cited therein). The early detection of an OFC is important to prevent high loads and for taking into account stringent structural design objectives (Goupil, 2010b; Alcorta-Garcia et al., 2011). Two types of OFCs are usually considered. The so-called *liquid failure* is an additive oscillatory fault signal inside the actuator positioning control loop. The *solid failure* involves an oscillatory signal which completely replaces a normal signal in the actuator positioning loop. According to Goupil (2010b), the relevant frequency range for the OFC is 0.1-10 Hz. The fault identification challenge for OFC is the need of an early detection, which imposes short detection times corresponding to a few oscillation periods. Another challenge is the detection of small amplitude oscillations of the control surfaces in the presence of measurement noise of comparable magnitudes. Finally, the fault detection and identification performance must be robustly achieved over the whole flight envelope, for various pilot maneuvers and wind conditions, and over the whole range of uncertain parameter variations.

In this paper we address the above challenges by proposing a complete methodology for the design of a dedicated model based *fault detection and diagnosis* (FDD) system, which allows the reliable early detection of OFC characterized by low amplitude oscillations in a given frequency range. The main factors which contributed to a satisfactory solution of the OFC identification problem are: (1) an accurate actuator modelling via simple *linear parameter-varying* (LPV) models; (2) an improved oscillation detection and frequency identification algorithm relying on a recursive formulation of the discrete Fourier transform; and (3) the integrated optimal tuning of the free parameters of the FDD system using multi-objective optimization techniques. Additionally, worst-case optimization-based search is used for robustness assessment of the resulting FDD system attached to the closed-loop flight control system. In what follows, we describe more in detail the above aspects and apply the proposed methodology for the identification of the OFC for an elevator surface actuator of a civil aircraft.

⋆ This work was performed in the framework of the ADDSAFE Project: Grant agreement no.: FP7-233815.

2. THE FDD SYSTEM FOR OFC IDENTIFICATION

The FDD system to be used to detect and identify different OFCs is depicted in Fig. 1, where besides the residual generator, blocks for residual evaluation, decision making and fault identification are present. The fault identification for the OFC involves the determination of the main characteristics of an oscillatory fault signal f from the generated residual signal r (e.g., via an estimate of the oscillation frequency) in the presence of noise signals $w(t)$.

The FDD system structure in Fig. 1 includes a residual generator for fault detection (or simply, a fault detector), which processes the commanded actuator position u and the measured current actuator position y and generates the scalar residual signal r. For the robust fault detection considered in this paper, a LPV gain-scheduled detector will be used, where ρ_2 is the vector of scheduling variables as described in Section 3. The residual evaluation block computes a specific approximation θ of the residual norm $||r||$. This value is used in the decision making block, where a threshold-based decision logic is employed to generate the decision signal i, which, if nonzero, triggers a signal based fault identification process. The output of the fault identification block is a classification signal c, which indicates the presence or absence of oscillations. This

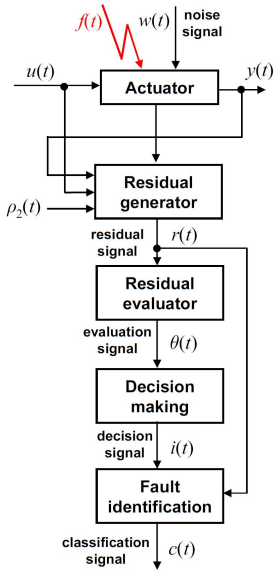

Fig. 1. FDD system for OFC monitoring

signal is crucial for triggering an adequate reconfiguration of the actuation system when the OFC occurs (e.g., switching to a backup actuator).

The employed model-based methodology for the design of the elements of the FDD system in Fig. 1 has the following main steps:

(1) Development of suitable LPV synthesis models of the underlying actuator;
(2) Synthesis of LPV residual generators for robust fault detection;
(3) Setting up of the residual evaluation and decision making blocks;
(4) Development of signal processing based fault identification schemes;
(5) The robustness assessment of the FDD system.

In what follows we describe these main steps and present an application of the proposed OFC identification techniques in the case of a civil aircraft elevator.

3. LPV MODEL GENERATION FOR THE NONLINEAR ACTUATOR MODEL

In this section we describe the development of a quasi-LPV approximate model for a system formed from an actuator and the associated control surface. For the details on the derivation of the quasi-LPV model see (Varga et al., 2011). The resulting actuator model has a first order LPV-system representation of the form

$$\begin{aligned} \dot{x} &= -k(\rho)x + k(\rho)u, \\ y &= x, \end{aligned} \tag{1}$$

where x and y are the rod position and u is the commanded position. The gain $k(\rho)$ generally depends on both measurable and unmeasurable parameters contained in a vector ρ. Typical values of the gain are around $k_0 = 14$.

The underlying actuator model is a simplified nonlinear dynamic model of an hydraulic servo controlled actuator described by a first order nonlinear state equation of the form (Goupil, 2010b; Márton and Ossmann, 2012)

$$\dot{x} = K_{ci}K_p(u-x)\sqrt{\frac{\Delta P(x) - \frac{F_{aero}(p,x,\dot{x}) + K_d\dot{x}^2}{S}}{\Delta P_{ref}}}, \tag{2}$$

where K_p is the servo control gain, K_{ci} is a gain to convert an estimated current to a corresponding rod speed, ΔP is the hydraulic pressure delivered to the actuator, ΔP_{ref} is a differential pressure for a fully opened servo-valve (maximum rod speed), F_{aero} represents the aerodynamic forces at the control surface, $K_d\dot{x}^2$ represents the estimated servo-control load of the adjacent actuator in damping mode and S is the actuator piston surface area. The components of the vector p are the calibrated airspeed V_{cas}, the aircraft altitude h, the aircraft mass m and the position of the center of gravity X_{cg} along the x-axis.

To get a simple quasi-LPV model approximating (2) with good accuracy, we approximated the nonlinear gain

$$K(p,x,\dot{x}) := K_{ci}K_p\sqrt{\frac{\Delta P(x) - \frac{F_{aero}(p,x,\dot{x}) + K_d\dot{x}^2}{S}}{\Delta P_{ref}}}$$

by an easily computable gain $k(p,x,\dot{x})$, which is then used in the first order actuator model as given in (1). The main variations of K are caused by the aerodynamic force F_{aero} that acts on the control surface, where F_{aero} itself usually depends on the parameters in p, the actuator position x and the sign of the actuator position rate $\dot{x}$. The effect of these variations is a reduction or increase of the gain, and thus variations of the response speed of the actuator.

Physical considerations as described in (Varga et al., 2011) led to choose $k(p,x,\dot{x})$ of the form

$$k(p,x,\dot{x}) = C_0(p) + C_1(p)\text{sign}(\dot{x})(x + C_2(p)) \tag{3}$$

where for fixed p, $C_0(p)$ can be interpreted as the nominal gain, $C_1(p)$ describes the influence of the deflection angle x on k, while the factor $\text{sign}(\dot{x})$ allows to distinguish between upward and downward movements of the control surface. $C_2(p)$ can be interpreted as a position offset. The chosen functional dependence on x and $\text{sign}(\dot{x})$ reflects the actual behavior of the actuator dynamics for different control surface positions and signs of deflection rate. For $C_i(p)$, $i = 0, 1, 2$, affine approximations have been used, where the intervening constant coefficients have been determined using parameter fitting techniques based on comparing the output responses of the nonlinear actuator model (2) and LPV-model (1). The final form of $k(\rho)$, with $\rho = (x, \text{sign}(\dot{x}), p)$ is simple enough to be used in LPV-model based fault diagnosis applications.

4. SYNTHESIS OF AN LPV RESIDUAL GENERATOR

Assume temporarily that the parameters in ρ are constant. In this case we can use an input-output representation of the actuator fault model in the form

$$\mathbf{y}(s) = G_u(s,\rho)\mathbf{u}(s) + G_f(s,\rho)\mathbf{f}(s), \tag{4}$$

where $\mathbf{y}(s)$, $\mathbf{u}(s)$, and $\mathbf{f}(s)$ are the Laplace-transformed quantities of $y(t)$, $u(t)$, and $f(t)$, respectively, and $G_u(s,\rho)$ and $G_f(s,\rho)$ are the corresponding parameter dependent transfer functions. $G_u(s,\rho)$ corresponding to (1) is

$$G_u(s,\rho) = \frac{k(\rho)}{s + k(\rho)} \tag{5}$$

while $G_f(s,\rho) = G_u(s,\rho)$ for an input located fault (assumed in this paper). For an output located fault we can alternatively use $G_f(s,\rho) = 1$.

Regarding the unknown parameter vector ρ, generally we can assume that it has two components: $\rho_1 \in \Pi_1$, which is not measurable, and $\rho_2 \in \Pi_2$, which is measurable, and thus $\rho \in \Pi := \Pi_1 \times \Pi_2$. In the case of the elevator actuator model, if the mass m and center of gravity position X_{cg} are not measurable, we can split ρ in $\rho_1 = (m, X_{cg}, \delta V_{cas}, \delta h)$ and $\rho_2 = (x, \text{sign}(\dot{x}), V_{cas}, h)$. Here, δV_{cas} and δh are uncertainties in the measurements of V_{cas} and h, respectively. However, if we can assume that m and X_{cg} can be estimated with a certain accuracy, then denoting with δm and δX_{cg} the estimation errors in the measured m and X_{cg}, respectively, we can choose $\rho_1 = (\delta m, \delta X_{cg}, \delta V_{cas}, \delta h)$ and $\rho_2 = (x, \text{sign}(\dot{x}), m, X_{cg}, V_{cas}, h)$.

As residual generator we use a parameter dependent filter of the form

$$\mathbf{r}(s) = Q(s, \rho_2) \begin{bmatrix} \mathbf{y}(s) \\ \mathbf{u}(s) \end{bmatrix}, \tag{6}$$

where $Q(s, \rho_2)$ is the 1×2 transfer-function matrix of the filter, which explicitly depends on the measurable parameter ρ_2 (e.g., via an equivalent state-space realization of the filter). For a physically realizable filter, $Q(s, \rho_2)$ must be robustly *stable*, having only poles with negative real parts for all values of ρ_2. The robust fault detection synthesis problem addresses the robustness of the fault detection system with respect to both the non-measurable parameter ρ_1 and measurable parameter ρ_2 by attempting to achieve robustness using an LPV gain scheduling approach.

To address the robust detection of OFC, we employed the synthesis method described in (Varga, 2011; Varga et al., 2011). Assuming all components of ρ entering in the model (5) are measurable (i.e., $\rho_2 = \rho$), we can use a first order detector of the form

$$Q(s, \rho) = \left[\frac{a}{k_0} \frac{s + k(\rho)}{s + a} \quad -\frac{k(\rho) a}{k_0 (s + a)} \right], \tag{7}$$

where a is an arbitrary positive value specifying the dynamics of the detector and k_0 is a typical nominal value of the gain $k(\rho)$. By replacing in (6) $\mathbf{y}(s)$ by its expression in (4), we obtain the internal form of the detector

$$\mathbf{r}(s) = R_u(s, \rho)\mathbf{u}(s) + R_f(s, \rho)\mathbf{f}(s) \tag{8}$$

where

$$[\, R_u(s, \rho) \,|\, R_f(s, \rho) \,] := Q(s, \rho_2) \left[\begin{array}{c|c} G_u(s, \rho) & G_f(s, \rho) \\ 1 & 0 \end{array} \right] \tag{9}$$

The choice (7) of $Q(s, \rho_2)$ guarantees an exact decoupling of control inputs in (9), thus $R_u(s, \rho) = 0$. The corresponding fault-to-residual transfer function is

$$R_f(s, \rho) = \frac{k(\rho)}{k_0} \frac{a}{s + a}$$

Thus, the residual signal provides a filtered estimation of the fault, allowing to easily reconstruct the actuator fault signal f for further use in fault identification.

The LPV state-space realization of the residual generator (6) can be always obtained in the form

$$\begin{aligned} \dot{x}_Q(t) &= A_Q x_Q(t) + B_Q(\rho) \begin{bmatrix} y(t) \\ u(t) \end{bmatrix} \\ r(t) &= C_Q x_Q(t) + D_Q(\rho) \begin{bmatrix} y(t) \\ u(t) \end{bmatrix} \end{aligned} \tag{10}$$

For the detector (7), the state-space matrices are

$$\begin{aligned} &A_Q = -a,\ B_Q(\rho) = a \left[\frac{k(\rho) - a}{k_0} \quad -\frac{k(\rho)}{k_0} \right], \\ &C_Q = 1, \quad D_Q = \left[\frac{a}{k_0} \quad 0 \right]. \end{aligned} \tag{11}$$

The chosen form (7) of the detection filter leads to a state-space realization with a constant feed-through matrix D_Q. This has the major advantage to prevent all direct effects on r of the discontinuities in the scheduling signal ρ_2 (e.g., jumps due to the presence of the signum-function in (3)).

5. SETUP OF RESIDUAL EVALUATION AND DECISION MAKING BLOCKS

5.1 Residual evaluation

The evaluation of the residual signal often requires the computation of a measure of the residual signal energy, for which the 2-norm of the signal is usually an appropriate choice. For this purpose, a so-called Narendra signal evaluation scheme can be used of the form

$$\theta(t) = \alpha |r(t)| + \beta \int_0^t e^{-\gamma(t-\tau)} |r(\tau)| d\tau, \tag{12}$$

where $\theta(t)$ can be generated by the first order differential equation

$$\begin{aligned} \dot{\xi}(t) &= -\gamma \xi(t) + \beta |r(t)| \\ \theta(t) &= \xi(t) + \alpha |r(t)|, \end{aligned} \tag{13}$$

The filter parameters $\alpha \geq 0$ and $\beta \geq 0$ are suitable weights for instantaneous and long-term values, respectively, while $\gamma > 0$ is the forgetting factor.

5.2 Decision making

The evaluation signal $\theta(t)$ is compared to a specific threshold J_{th} in the decision making process to determine the decision signal $i(t)$ using the decision logic

$$\begin{aligned} \theta(t) < J_{th} &\Rightarrow i(t) = 0 \Rightarrow \text{no fault} \\ \theta(t) \geq J_{th} &\Rightarrow i(t) = 1 \Rightarrow \text{fault} \end{aligned} \tag{14}$$

The signal $\theta(t)$ is ideally equal to zero or sufficiently small in fault free situations, whereas it shall exceed the threshold J_{th} when a fault occurs in the system. Hence, the appropriate selection of the values of the free parameters α, β or γ, together with an appropriate threshold J_{th} essentially influences the performance of the FDD system.

The setup of the parameters (α, β, γ) of the evaluation blocks and the threshold J_{th} used in the decision blocks must ensure that the requirements regarding typical performance criteria used in the industry as the *false alarm rate* (FAR), the *missed detection rate* (MDR) or the *detection time performance* (DTP) are fulfilled. A multi-objective optimization-based parameter tuning approach aiming the simultaneous minimization of all these quantities can be employed. For the minimization of these criteria, function evaluations based on extensive simulations of the closed-loop aircraft augmented with an FDD system are necessary to determine worst-case combinations of unknown external signals (e.g., pilot inputs u_p, wind disturbances d) and various parametric uncertainties $\rho \in \Pi$. Unfortunately, for arbitrary external signals these function evaluations involving global optimizations in function spaces are hardly computationally tractable.

To overcome this computational bottleneck, instead of arbitrary external signals, we used bounded input signals in given finite classes $u_p \in \mathcal{U}$, $d \in \mathcal{D}$ and $f \in \mathcal{F}$, where $\mathcal{U}$ includes several meaningful pilot maneuvers, $\mathcal{D}$ consists of random wind inputs of given maximum amplitude, and $\mathcal{F}$ includes oscillatory fault signals (liquid and solid) with given amplitudes and frequencies.

5.3 Determination of detection threshold

The approach used in this paper aims to completely avoid false alarms and missed detections. For this, for appropriately chosen values of parameters (α, β, γ) (e.g., determined by a preliminary optimization-based tuning) we determine a value of the decision threshold J_{th} to ensure FAR = 0 and MDR = 0.

Consider the *false alarm bound* defined as

$$J_{th}^f = \sup_{\substack{\rho \in \Pi \\ u_p \in \mathcal{U} \\ d \in \mathcal{D} \\ f = 0}} \max_{t \le t_{fin}} \theta(t) \tag{15}$$

where t_{fin} is the duration of the maneuvers in $\mathcal{U}$. To avoid false alarms, the threshold J_{th} used in the decision block must be chosen such that $J_{th} > J_{th}^f$.

Similarly, consider the *detection bound* defined as

$$J_{th}^d = \inf_{\substack{\rho \in \Pi \\ u_p \in \mathcal{U}_j \\ d = 0 \\ f \in \mathcal{F}}} \max_{t \le t_{detec}} \theta(t) \tag{16}$$

Here, $\mathcal{U}_j \subset \mathcal{U}$ is a subclass of pilot inputs used for a specific maneuver during which the fault $f \in \mathcal{F}$ occurs and has to be detected within a specified detection time t_{detec}. To avoid missed detection, the threshold J_{th} used in the decision block must be chosen such that $J_{th} < J_{th}^d$.

For the computation of J_{th}^f and J_{th}^d, solving global worst-case optimization problems to find the worst-case parameter combinations appears to be the most adequate choice. However, less demanding computational approaches can be used, as a gridding based worst-case search over the flight envelope and parameter space, or Monte-Carlo simulations, to determine approximations of the upper bound J_{th}^f and lower bound J_{th}^d.

A positive *detection gap* $J_{th}^d - J_{th}^f$ can be interpreted as a robustness measure of the fault detection performance. Note that the worst-case parameter combinations resulting from the computation of J_{th}^f in (15) and J_{th}^d in (16) are usually different. If $J_{th}^d - J_{th}^f > 0$, a *constant* threshold J_{th} satisfying $J_{th}^d \le J_{th} < J_{th}^f$ can be chosen to guarantee *no false alarms* and *no missed detections*. A choice of J_{th} near to J_{th}^f allows in general shorter detection times and smaller detectable fault amplitudes.

The detection time of a fault f can be determined as

$$t_d = \min_{t \le t_{fin}} \{\, t \mid \theta(t) > J_{th} \}. \tag{17}$$

In our study, for an OFC with frequency ω, we target an overall detection time not larger than three periods $t_{detec} = \frac{6\pi}{\omega}$.

6. IDENTIFICATION OF OFC

By using a sufficiently accurate LPV approximation (1) of the actuator nonlinear model (2) as basis for residual generator synthesis, the resulting residual signal r will contain the same oscillatory components as the fault signal. Once the occurrence of a fault has been detected using the decision logic (14), the fault identification stage follows aiming to detect the presence of oscillations in r in the relevant frequency band. For the identification of OFC, a signal processing based technique has been proposed by Goupil (2010b), which involves sub-band filtering of the residual signal followed by an oscillation counting. Separate schemes are used to identify liquid and solid type OFCs. In this section, we describe an alternative approach, with a sound mathematical basis and which is easily implementable on-board. The proposed approach needs no special treatment of different types of OFCs.

A rigorous approach to identify oscillations in noise corrupted signals is the periodogram method (P. Stoica and R. L. Moses, 1997), which is based on determining the power spectrum of a signal using the *discrete Fourier transform* (DFT). The DFT is easily computable using the *fast Fourier transform* (FFT) algorithm and allows a satisfactory accurate evaluation of the oscillation frequency together with strong statistical guarantee of the presence of the oscillatory signal. Still, the on-board implementation of FFT-based frequency analysis is questionable, due to the strict code certification requirements.

To overcome these limitations, a recursive version of the DFT, as described in (Morelli, 2000), can be used to detect oscillations in real-time. Let T_s be the sampling period and let N be the expected length of the time series $r(t_i)$, for $t_i = iT_s$, for $i = 0,\ 1, \ldots, N-1$. The DFT computes

$$X(\omega) := \sum_{i=0}^{N-1} r(t_i) e^{-j\omega t_i}$$

for a given frequency ω. The computation of $X(\omega)$ can be done recursively by defining the partial sum

$$Y_k(\omega) = \sum_{i=0}^{k} r(t_i) e^{-j\omega t_i}$$

and observing that

$$Y_k(\omega) = Y_{k-1}(\omega) + r(t_k) e^{-j\omega t_k} \tag{18}$$

for $k = 1, \ldots, N$. Evidently, $X(\omega) = Y_{N-1}(\omega)$, where the iteration (18) is initialized with $Y_0(\omega) = 0$. An oscillation of frequency nearby to ω is detected at iteration K if $|Y_K(\omega)| > J_{th,freq}$, where $J_{th,freq}$ is a suitable threshold. The main appeal of this approach is that usually $K \ll N$, thus fast detection of the presence of oscillations nearby a frequency ω is possible.

For the choice of the threshold $J_{th,freq}$, we can employ the expression $J_{th,freq} = \frac{N}{2} J_n$, where $J_n < 1$ is a normalized threshold for unit amplitude sinusoidal signals of frequency ω. The value of J_n generally accounts for the need to avoid undetected oscillations of frequency ω_x nearby ω. Recall that the frequency resolution of the DFT for N samples and a sampling period T_s is $\frac{2\pi}{T_s N}$, and therefore the frequency bin around ω contains all frequencies ω_x such that $|\omega_x - \omega| \le \frac{\pi}{T_s N}$. The magnitude of the resulting

Fourier coefficient for a unit amplitude sinusoidal signal of frequency ω_x is

$$|X(\omega)| = \frac{1}{2}\left|\frac{\sin[(\omega_x-\omega)NT_s/2]}{\sin[(\omega_x-\omega)T_s/2]}\right| \leq \frac{N}{2}$$

The maximum magnitude drop within a frequency bin results for $\omega_x = \omega \pm \frac{\pi}{T_s N}$ as

$$|\underline{X}(\omega)| = \frac{1}{2}\frac{1}{\left|\sin\frac{\pi}{2N}\right|}$$

Since $|\underline{X}(\omega)|/(N/2) > 2/\pi$ for all N, we can safely take $J_n = 2/\pi$ a safe threshold for each frequency bin.

Using the above choice for J_n, we can easily determine the minimum number of frequency values such that the union of the associated frequency bins covers the relevant frequency domain. Let $\Omega = \{\omega_1, \omega_2, \ldots, \omega_M\}$ be the frequency grid to be chosen with $\omega_1 > \omega_2 > \ldots > \omega_M$. Each ω_ℓ is the midpoint of an interval $\mathcal{I}(\omega_\ell) := [\underline{\omega}_\ell, \overline{\omega}_\ell]$, which defines a frequency bin with a resolution of $\frac{2\pi}{N(\omega_\ell)T_s}$, where $N(\omega_\ell)$ is the corresponding number of samples (to be chosen). The choice of these intervals must ensure that their reunion $\cup_{i=1}^{M}\mathcal{I}(\omega_\ell)$ fully covers the relevant frequency domain for the OFC. A non-overlapping choice is always possible by imposing $\overline{\omega}_\ell = \underline{\omega}_{\ell-1}$, and results by choosing $\underline{\omega}_\ell$ for $\ell = 1, 2, \ldots, M$ according to

$$\underline{\omega}_\ell = \frac{\underline{\omega}_{\ell-1}}{2}, \tag{19}$$

where $\underline{\omega}_0$ is the maximum frequency in the relevant frequency domain. $N(\omega_\ell)$ can be chosen to satisfy the worst-case detection time requirement of two periods for the maximum frequency in the ℓ-th bin $\overline{\omega}_\ell = \underline{\omega}_{\ell-1}$, that is, $N(\omega_\ell)T_s = 4\pi/\underline{\omega}_{\ell-1}$. For this choice, taking into account (19), we have the simple relations $N(\omega_\ell) = 2N(\omega_{\ell-1})$ between two successive numbers of samples. For example, using the above approach, the frequency domain $[0.15, 10]$Hz can be covered using a grid of $M = 6$ frequencies

$$\Omega = 2\pi \times \{7.5, 3.75, 1.875, 0.9375, 0.4687, 0.2343\}$$

and the corresponding values $\{20, 40, 80, 160, 320, 640\}$ of $N(\omega_\ell)$ for a typical sampling period of $T_s = 0.01$s.

The recursive algorithm (18) can be implemented efficiently and thus is appealing for real-time applications. Since usually $M \ll N$, we can discard the computations for $N - M$ frequency values of no interest (which would be automatically produced when employing the FFT). For increased efficiency, we can use the precomputed quantities $W(\omega) = e^{-j\omega T_s}$ for each $\omega \in \Omega$ and exploit that

$$s_k := e^{-j\omega t_k} = W(\omega)e^{-j\omega t_{k-1}} = W(\omega)s_{k-1} \tag{20}$$

Thus, at each step $k > 2$ we have to compute for each $\omega \in \Omega$ successively

$$\begin{aligned} s_k &= W(\omega)s_{k-1} \\ Y_k(\omega) &= Y_{k-1}(\omega) + r(t_k)s_k \end{aligned}$$

These iterations are initialized with $Y_1(\omega) = r(t_0)$ and $s_1 = 1$. Taking into account that the intervening $r(t_k)$ in (18) is a real quantity, the number of *floating point operations* (*flops*) to compute $Y_k(\omega)$ and update s_k is 1 complex and 2 real multiplications and 1 complex addition (equivalent to 6 real multiplications and 2 real additions). Thus, the operations at each step involve $8M$ *flops*. Finally, we stop iterating if an oscillation has been detected at a certain iteration k_{detec}. The total number of operations is about $8M(k_{detec} - 1)$ *flops*.

7. FDD SYSTEM TUNING AND ASSESSMENT

In this section we describe the application of the methodology described in Section 2 to the OFC detection of an elevator surface controlled by a hydraulic actuator. The nonlinear actuator model of the elevator is part of a nonlinear model of a closed-loop aircraft including a nonlinear control law ensuring robust stability over the whole flight envelope. For tuning and assessment purposes, the closed-loop aircraft model has been augmented with an FDD system as in Fig. 1, which includes the LPV residual generator determined in Section 4.

For the tuning of the FDD system, the values of the parameters (α, β, γ) of the residual evaluation block and the threshold J_{th} of the decision making block have been determined by maximizing the detection gap $J_{th}^d - J_{th}^f$. The optimal setting with $\alpha = 0.85$, $\beta = 0.8$, $\gamma = 0.08$ and $J_{th} = 0.7$ leads to a completely satisfactory fault detection performance. The signal processing based identification of the OFC frequency presented in Section 6 is triggered by the threshold crossing of the evaluation signal $\theta(t) > J_{th}$.

The robustness of the designed FDD system has been thoroughly tested for both fault free and faulty situations in the whole flight envelope and full range of aircraft parameter variations. To check for the lack of false alarms, typical maneuvers as for example, piloted flights with various pilot inputs (longitudinal/lateral stick doublets, pedal input demand, nose up/nose down demands) or typical navigation maneuvers (level flight, flight path angle target mode, yaw angle target mode, speed change, steady sideslip, coordinated turn, etc.) have been used.

Using optimization-based worst-case search, the *normalized detection time*

$$\vartheta_{det} = \sup_{\substack{\rho\in\Pi \\ u\in\mathcal{U}_j \\ d\in\mathcal{D} \\ f\in\mathcal{F}}} \frac{t_{id} - t_f}{t_{detec}} \tag{21}$$

has been used as clearance criterion, where t_f is the time of occurrence of the fault and t_{id} the time of the identification of OFC. A maximum value above 1 of this criterion indicates a violation of the required detection time t_{detec}.

A typical fault-free maneuver is depicted in Fig. 2, where the actuator output y follows almost instantly the demanded signal u. The generated residual r is corrupted only by the measurement noise in y, which is also present in the evaluation signal θ. This however remains below the threshold J_{th}, indicating no fault.

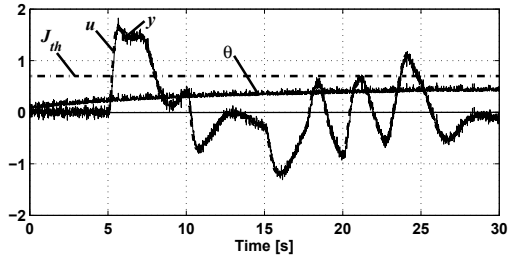

Fig. 2. Example for fault free maneuvering

Fig. 3 illustrates the occurrence of a liquid OFC with a frequency of 0.5Hz (i.e., $\omega = \pi$) in the actuator output y at t_f. The visible difference between u and y indicates that the residual signal has likely an oscillatory behavior. Indeed, the evaluation signal θ increases rapidly and crosses the threshold J_{th} at t_d, when the fault is detected. The signal based fault identification indicates at t_{id} that the value $|Y_k(\pi)|$ of the power spectral density of the residual becomes larger than the threshold $J_{th,freq}$. In this example the total detection time of the OFC is $t_{id} - t_f = 2.6$ seconds, of which $t_d - t_f = 0.4$ seconds are required to detect the occurrence of a fault and $t_{id} - t_d = 2.2$ seconds to identify it. Thus, only 1.3 periods of the targeted 3 periods are necessary to identify this OFC.

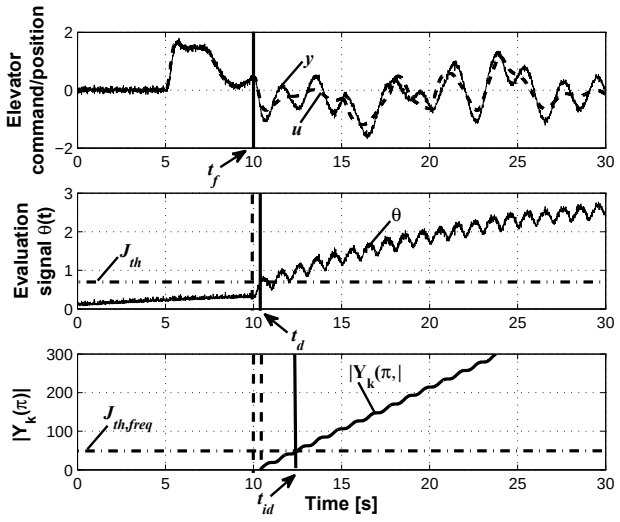

Fig. 3. Detection and identification of an OFC

To assess the global performance of the FDD system for the detection of the OFC, the worst-case normalized detection time ϑ_{det} defined in (21) has been determined for several OFC situations in a cruise flight. Recall that the specific choice of the threshold J_{th} described in subsection 5.3 already guarantees the fulfillment of all requirements regarding the lack of false alarms and missed detections, as well as satisfactory detection times. Thus, the performed worst-case analysis only provides supplementary information on the overall robustness of the detection time performance of the FDD system. The worst-case analysis results for three liquid and three solid OFCs for the frequencies 0.5Hz, 1.5Hz, and 7Hz are listed in Table 1. As it can be observed, the normalized detection times tend to increase with the frequency, which indicates that the detection of OFC at higher frequencies appears to be more challenging for the proposed method.

Table 1. Worst-case analysis results

OFC Type	OFC frequency	t_{detec}	$t_{id} - t_f$	ϑ_{det}
Liquid	0.5Hz	6s	3.72s	0.62
Solid	0.5Hz	6s	3.54s	0.59
Liquid	1.5Hz	2s	1.36s	0.68
Solid	1.5Hz	2s	1.26s	0.63
Liquid	7Hz	0.42s	0.34s	0.82
Solid	7Hz	0.42s	0.32s	0.75

8. CONCLUSIONS

In this paper we proposed a model-based synthesis, tuning and assessment methodology for the development of an FDD system for the early detection of OFC for aircraft actuators. The main features of the proposed approach, which confer a superior performance compared to existing approaches, are: (1) relying on accurate LPV models allowing high performance detector synthesis; (2) application of advanced synthesis methods of LPV residual generators guaranteeing robust and fast fault detection; (3) employing an integrated optimization-based tuning of the parameters of the fault evaluation and decision making blocks, including the determination of detection thresholds, to guarantee *no false alarms* and *no missed detections*; (5) employing theoretically sound, but still real-time implementable fault identification method; and (6) employing worst-case search based on global-optimization for robustness assessment. An important aspect to mention is that while the synthesis of the LPV residual generator relies on a fault monitoring approach at component (actuator) level, the tuning of the overall FDD system parameters and the final robustness analysis involve the closed-loop aircraft. The proposed methodology has been successfully applied for the design of an FDD system for the identification of the solid and liquid OFCs of an elevator actuator. The strong requirements for no false alarms, no missed detections and short fault detection times have been completely fulfilled in the presence of parametric uncertainties over the whole range of envelope values and of significant parametric uncertainties and measurement noise.

REFERENCES

Alcorta-Garcia, E., Zolghadri, A., and Goupil, P. (2011). A nonlinear observer-based strategy for aircraft oscillatory failure detection: A380 case study. *IEEE Transactions on Aerospace and Electronic Systems*, 47, 2792 – 2806.

Goupil, P. (2010b). Oscillatory failure case detection in the A380 electrical flight control system by analytical redundancy. *Control Engineering Practice*, 18, 1110–1119.

Márton, L. and Ossmann, D. (2012). Energetic approach for control surface disconnection fault detection in hydraulic aircraft actuators. *Proc. of SAFEPROCESS'12, Mexico City, Mexico.*

Morelli, E.A. (2000). Real-time parameter estimation in the frequency domain. *AIAA Journal of Guidance, Control and Dynamics*, 23, 812–818.

P. Stoica and R. L. Moses (1997). *Introduction to Spectral Analysis.* Prentice Hall.

Varga, A. (2011). On parametric solution of fault detection problems. *Proc. IFAC 2011 World Congress, Milano, Italy.*

Varga, A., Hecker, S., and Ossmann, D. (2011). Diagnosis of actuator faults using LPV-gain scheduling techniques. *Proc. of AIAA Guidance, Navigation, and Control Conference, Portland, Oregon, USA.*